JOURNAL OF CHEMICAL INFORMATION AND MODELING

Article

pubs.acs.org/jcim

Molecular Determinants of Bim(BH3) Peptide Binding to Pro-Survival Proteins

Laura Delgado-Soler, Marta Pinto, Kaori Tanaka-Gil, and Jaime Rubio-Martinez*

Department of Physical Chemistry, University of Barcelona and the Institut de Recerca en Quimica Teorica i Computacional (IQTCUB), Barcelona, Spain

Supporting Information

ABSTRACT: Proteins of the Bcl-2 family regulate apoptosis through the formation of heterodimers between antiapoptotic or pro-survival proteins and proapoptotic or pro-death proteins. Overexpression of antiapoptotic proteins not only contributes to the progression of many cancers, but also confers resistance to the chemo- and radiotherapeutic treatments. It has been demonstrated that peptides containing the BH3 domain of proapoptotic Bcl-2 family members are able to bind and inhibit antiapoptotic proteins. For this reason, the design of small molecules mimicking the BH3 domain of proapoptotic proteins has emerged as a promising therapeutic strategy for cancer treatment during the last years. However, BH3 domains exhibit different affinities for binding to antiapoptotic proteins; whereas Bim(BH3) and Puma(BH3) are able to bind all antiapoptotic proteins, others like Bad(BH3) and Bmf(BH3) show preference for some proteins over others. Consequently, the ability of a BH3-mimetic to kill tumor cells will depend on the BH3 peptide used as template and thus will have a selective or pan-inhibition effect. Recently, it has been suggested that this last approach could be interesting. Therefore, the present work is aimed to elucidate how the nonselective peptide Bim(BH3) is able to bind to all of the Bcl-2 family antiapoptotic proteins. To unravel the molecular determinants of this pan-inhibition, we used the MM-PB/GBSA approaches to calculate the binding free energy of the different complexes studied and to determine which residues of the peptide have the largest contribution to complex formation. Results obtained in the present work show that the binding of Bim(BH3) to pro-survival proteins is mainly hydrophobic and that specific interactions are fully distributed along the peptide sequence.

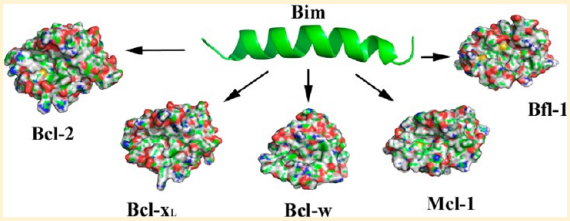

INTRODUCTION

Proteins of the Bcl-2 family are one of the most important regulators of apoptosis. These proteins can promote either cell survival (called antiapoptotic proteins such as Bcl-x_L, Bcl-2, Bcl-w, Mcl-1, and Bfl-1) or cell death (called proapoptotic proteins such as Bad, Bak, Bax, Bid, Bik, Bim, Hrk, Noxa, or Puma) and are characterized by sharing at least one region of sequence homology termed Bcl-2 homology (BH) and numbered from 1 to 4 (BH1−BH4).[1]

It has been postulated that evasion of apoptosis is a requirement for oncogenesis.[2,3] One of the ways by which cancer cells can achieve this is by up-regulation of pro-survival Bcl-2 family members. Consequently, abrogating the anti-apoptotic function of these pro-survival proteins has emerged during the last years as a promising therapeutic strategy for cancer treatment.[4]

Although the precise mechanism by which this family of proteins regulates apoptosis is still poorly understood, it is well accepted that anti- and proapoptotic proteins modulate their opposite functions through heterodimerization.[5] The experimental structures of antiapoptotic proteins complexed with peptides derived from the BH3 domain of proapoptotic proteins have provided the first insights into the molecular mechanism of the heterodimerization of this family of proteins. In these complexes, the antiapoptotic protein forms a hydrophobic cleft on its surface wherein the hydrophobic face of an amphipathic α-helix containing the BH3 domain of the proapoptotic protein binds.[6−8] In this scenario, it was postulated that small molecules mimicking the BH3 α-helix of proapoptotic proteins may be able to bind to the same hydrophobic groove of antiapoptotic Bcl-2 family members, blocking their heterodimerization and leading to apoptosis. This strategy has been fully supported by experimental evidence showing the ability of short synthetic peptides comprising the BH3 domain of proapoptotic proteins to bind and inhibit antiapoptotic proteins promoting apoptosis.[7,9−12] Since then, several BH3-mimetics have been reported, although still there is none available for clinical use.[13]

One of the most important considerations to bear in mind when designing BH3 mimetics is the different affinity of BH3 domains for individual antiapoptotic proteins. While certain BH3 domains such as Bim(BH3) or Puma(BH3) bind to all pro-survival proteins, others like Bad(BH3) or Bmf(BH3) bind preferentially Bcl-x_L, Bcl-2, and Bcl-w, whereas Noxa(BH3) prefers Mcl-1 and Bfl-1.[14] Consequently, the therapeutic effects observed for a BH3-mimetic will clearly depend on the BH3 peptide used as a template. A proof of this concept has been

Received: March 29, 2012
Published: July 15, 2012

provided by the discovery of ABT737. This compound was developed by Abbott in a rational design process devoted to inhibit both Bcl-xl and Bcl-2 proteins.[15] The functional characterization of ABT737 showed that this compound is functionally mimetic to Bad(BH3), being able to bind Bcl-x_L, Bcl-2, and Bcl-w with high affinity but not Mcl-1 or Bfl-1.[16] Consequently, the efficacy of this compound is restricted to cells in which Mcl-1 is not overexpressed.[16,17] These findings evidence the need to target more than one Bcl-2 pro-survival proteins to obtain an effective cancer therapy. Hence, in the last years, there is a growing interest in developing new anticancer agents able to bind and inhibit the pro-survival Bcl-2 family members in the same manner as do Bim(BH3) or Puma(BH3). However, although important advances have been carried out from an experimental perspective to design peptides with pronounced selectivity for some members of the Bcl-2 protein family,[18] no theoretical calculations describing the molecular determinants of selective binding between Bcl-2 family members have been reported.

In this scenario, the aim of the present work is to provide the molecular determinants of the Bim(BH3) binding to the antiapoptotic proteins Bcl-x_L, Bcl-2, Bcl-w, Mcl-1, and Bfl-1 (hereafter referred to as X). The selection of this peptide was based on the following considerations: (1) the ability of Bim(BH3) to bind all five antiapoptotic proteins with similar affinities has been previously demonstrated;[14,18] (2) previous experimental studies have shown the ability of this peptide to induce apoptosis as efficiently as when BH3-only proteins with complementary binding profiles are used;[14] and (3) high-resolution structures for the antiapoptotic proteins Bcl-x_L, Mcl-1, and Bfl-1 complexed with Bim(BH3) are available in the Protein Data Bank. Results obtained from the present work should be valuable in the development of new anticancer agents able to target Bcl-x_L, Bcl-2, Bcl-w, Mcl-1, and Bfl-1. The ability of these agents to inhibit a broad spectrum of antiapoptotic proteins can contribute to the development of new compounds, allowing one to study the real pharmacological effects of Bim-like compounds.

METHODS

Preparation of the X/Bim(BH3) Complexes. Three-dimensional structures of the Bcl-x_L/Bim(BH3),[19] Mcl-1/Bim(BH3),[20] and Bfl-1/Bim(BH3)[21] complexes were extracted directly from the Protein Data Bank (PDB) (http://www.rcsb.org/pdb) (PDB codes: 3FDL, 2PQK, and 2VM6, respectively). Loop residues not resolved in the Mcl-1/Bim(BH3) crystal structure were extracted from the complex formed by this protein and a Bim-derived Mcl-1 selective BH3 ligand (PDB code 2NLA).[22] Similarly, unresolved residues of the Bfl-1/Bim(BH3) complex were modeled using the Mcl-1/Bim(BH3) equivalent residues.

No structural information was available in the PDB for the Bcl-2/Bim(BH3) and Bcl-w/Bim(BH3) complexes. In the case of the Bcl-2 protein, given that this protein shares a 47% amino acid sequence identity with Bcl-x_L, the Bcl-2/Bim(BH3) complex was modeled by homology with Modeler 9v3[23,24] using the crystal structure of the Bcl-x_L/Bim(BH3) complex (PDB code 3FDL) as a structural template. Similarly, the three-dimensional structure of the Bcl-w/Bim(BH3) complex was generated by homology to the crystallographic complex Bcl-w/Bid(BH3)[25] (PDB code 1ZY3).

The five X/Bim(BH3) complexes were superimposed using the backbone heavy atoms to eliminate the highly unstructured terminal residues of peptide and protein not present in all five structures. Missing atoms were added in standard positions using the *leap* module of the AMBER v.9 software package.[26] Next, each complex was placed in a cubic periodic box filled with TIP3P water molecules,[27] imposing a minimal distance of 15 Å between the solute and the box walls. Water molecules closer than 1.8 Å to any complex atom were removed. Next, neutralizing counterions were added to each one of the systems at positions of lowest electrostatic potential using the *leap* module of AMBER.

Molecular Dynamics of the X/Bim(BH3) Complexes. Prior to molecular dynamics (MD) simulations, each system was first relaxed. Energetic minimizations were carried out using the AMBER ff99SB force field[28] and the *pmemd* module of the AMBER v.9 program suite. Minimizations were performed in a multistep procedure: (1) minimization of the water molecules and ions trough 5000 steps of the steepest descent algorithm keeping fixed the rest of the system; (2) relaxation of the modeled residues in three consecutive stages, each of them consisting of 5000 steps of the steepest descent method and using a decreasing force constant of 50, 5, and 0.5 kcal/mol Å, respectively; (3) minimization of the side chains of the whole complexes by means of 5000 steps of the steepest descent optimization and the same constraints for the heavy backbone atoms of peptide and protein as those employed in the previous step for the modeled residues; and finally (4) minimization of the whole complexes without restrictions by using 5000 steps of the steepest descent method followed by 5000 of conjugate gradient.

Minimized complexes were used as starting points for MD simulations. Trajectories were carried out at 300 K by coupling the system to a thermal bath using the Berendsen algorithm[29] with a time coupling constant of 0.2 ps. All bonds involving hydrogen atoms were constrained to their equilibrium value using the SHAKE algorithm,[30] allowing the use of a 2 fs time step in all of the simulations. Nonbonded interactions were truncated using a cutoff of 10 Å, and long-range electrostatic interactions were treated with the particle-mesh Ewald summation.[31]

After minimization, structures were heated stepwisely at a rate of 30 K every 10 ps, maintaining all backbone atoms constrained to their initial positions with a force constant of 0.1 kcal/mol·Å. Once the systems were heated, a 10 ps simulation at constant pressure (NPT ensemble) without any restraint was performed for density equilibration with a time constant for heat bath coupling of 1 ps. Systems then were equilibrated for 5 ns within the NVT assemble to allow structural readjustments (equilibration stage). After equilibration, 50 ns of molecular dynamics was performed on each system to ensure their energetic convergence. Only the last 5 ns of each trajectory was considered for data collection (production stage).

Binding Free Energy Calculations. Free energies of binding were calculated using the Molecular Mechanics Poisson−Boltzmann Surface Area (MM-PBSA) and the Molecular Mechanics Generalized Born Surface Area (MM-GBSA) algorithms as implemented in the AMBER package.[32] For each one of them, the binding free energy can be evaluated according to the equation:

$$\Delta G_{\text{binding}} = \Delta G^{\text{gas}} + \Delta G^{\text{solv}} - T\Delta S$$

where ΔG^{gas} is the gas-phase interaction energy calculated by summing the internal energy (as strain energies from covalent

Table 1. Contribution of the Different Energy Terms and Absolute Binding Free Energies (kcal/mol) of the Different X/Bim(BH3) Complexes, with X Being the Pro-Survival Proteins Bcl-x_L, Bcl-2, Bcl-w, Mcl-1, and Bfl-1, in the Last 5 ns of Molecular Dynamics[a]

	X				
	Bcl-x_L	Bcl-2	Bcl-w	Mcl-1	Bfl-1
ΔH_{vdW}	−116.21	−110.81	−117.38	−109.09	−103.80
ΔH_{ee}	−85.21	−106.88	−269.87	−156.81	−178.57
$\Delta G_{polar,PB}$	100.98	125.16	304.34	187.69	216.31
$\Delta G_{nonpolar,PB}$	−13.49	−13.28	−14.18	−11.85	−12.28
$\Delta G_{polar,GB}$	110.58	129.69	306.61	191.82	221.28
$\Delta G_{nonpolar,GB}$	−11.52	−11.36	−12.11	−10.01	−10.37
$\Delta G_{PB,total}$	−113.93	−105.80	−97.09	−90.06	−78.35
$\Delta G_{GB,total}$	−102.36	−99.35	−92.76	−84.09	−71.46
$-T\Delta S$	50.26	49.22	53.69	45.74	54.15
ΔG_{PB}	−63.67	−56.58	−43.40	−44.32	−24.20
ΔG_{GB}	−52.10	−50.13	−39.07	−38.35	−17.31
K_i (nM)	1.3 ± 0.4	1.4 ± 0.6	2.1 ± 0.3	1.9 ± 0.3	2 ± 0.1

[a]In this table, ΔH_{vdW} and ΔH_{ee} are the van der Waals and electrostatic mechanic energies; ΔG_{polar} and $\Delta G_{nonpolar}$ represent the electrostatic and nonpolar contributions to the solvation free energy, respectively, and $\Delta G = \Delta G_{total} - T\Delta S$, calculated using the MM-PBSA and MM-GBSA approaches. Experimental K_i values were obtained from Dutta et al.[18]

bonds and torsion angles) with noncovalent van der Waals (ΔH_{vdW}) and electrostatic (ΔH_{ele}) molecular mechanics energies. ΔG^{solv} is computed as the sum of polar (ΔG_{polar}) and nonpolar ($\Delta G_{nonpolar}$) terms. ΔG_{polar} can be calculated by numerically solving the Poisson−Boltzmann (PB) equation or by using a simplified form, the Generalized Born (GB) method, for the MM-PBSA and MM-GBSA algorithms, respectively. $\Delta G_{nonpolar}$ is calculated using the equation $\Delta G_{nonpolar} = \gamma SASA + \beta$, where SASA is the solvent-accessible surface area. ΔS is the entropic term accounting for the conformational entropy change of the two binding partners upon complexation.

In the present work, binding free energies of the X/Bim(BH3) complexes were calculated from a single molecular dynamics trajectory using the MM-PBSA and the MM-GBSA algorithms as implemented in AMBER v.9. The polar contribution of the solvation free energy was calculated by GB using the parameters developed by Onufriev et al.[33] and by PB with the *pbsa* program[34] of the same package. The values of the interior and exterior dielectric constants were set to 1 and 80, respectively. The solvent-accessible surface area was calculated using the LCPO method.[35] The values for γ and β constants were set to 0.00542 kcal/mol·Å^2 and −0.92 kcal/mol in the MM-PBSA calculation[32] and to 0.005 kcal/mol·Å^2 and 0 kcal/mol in the MM-GBSA approach.[36] Energy values were averaged over 500 snapshots extracted at time interval of 10 ps from the last 5 ns of each trajectory after ensuring that each one of these trajectories was completely stable.

Because of the computational requirements, entropic contributions were averaged over 50 snapshots extracted at a time interval of 100 ps from the last 5 ns of each trajectory using the MMPBSA.py module of AMBER v.11 within the harmonic approximation.

Multiple Molecular Dynamics. Binding free energies for the X/Bim(BH3) complexes were also calculated as average values of five binding free energies obtained from five 10 ns molecular dynamics trajectories using as starting points the minimized structures and with the MM-PBSA and the MM-GBSA algorithms described before. Energy values were averaged over 1000 snapshots extracted at time interval of 10 ps from the complete trajectory. Entropic contribution obtained using the long trajectories was used here.

Free Energy Decomposition. The contribution of each Bim(BH3) peptide residue to the binding free energy of each complex was analyzed using the MM-GBSA decomposition protocol[37] encoded in the *mm_gbsa* module of AMBER v.9. It was carried out using the GB approach to calculate the electrostatic component of the solvation energy and the LCPO for the nonpolar one. All energy components were calculated using the snapshots corresponding to the last 5 ns extracted as in the binding free energy calculations.

Analysis of the Molecular Dynamics Simulations. The hydrogen bonds between the protein X and the peptide Bim(BH3) were characterized using the *ptraj* module of AMBER. The occupancy of these bonds was calculated over the last 5 ns of simulation time, and only hydrogen bonds with occupancies greater or equal to 60% were considered. The criteria used for hydrogen bonding were hydrogen acceptor−donor atom distances of less than 3.5 Å and acceptor−H−donor angles of more than 120°. Water-bridged hydrogen bonds were also investigated with the same distance cutoff and angle cutoff values.

RESULTS AND DISCUSSION

The present study was aimed to obtain a better understanding of the features that allow Bim(BH3) to bind in a promiscuous manner to the antiapoptotic proteins Bcl-x_L, Bcl-2, Bcl-w, Mcl-1, and Bfl-1. To this end, the binding free energy of each X/Bim(BH3) complex was calculated using the MM-PBSA and MM-GBSA approaches. Detailed binding free energies between each X and residues of Bim(BH3) were calculated using a per-residue basis decomposition method. For the discussion, it will be only considered residues of peptide that have a contribution to the binding free energy of each complex equal to or lower than −1.2 kcal/mol.

Total Binding Free Energy of the X/Bim(BH3) Complexes. First, to determine the simulations convergence and the stability of the different complexes, the total binding free energy calculated by either the MM-PBSA or the MM-GBSA approach was plotted as a function of the trajectory length. As can be seen in Supporting Information Figure S1, different complexes have different $\Delta G_{binding}$ behavior along the molecular dynamics progression. One the one hand, Bcl-x_L/

Table 2. Total Solvation Free Energy (kcal/mol), Including the Entropic Contribution, Calculated with the MM-PBSA and MM-GBSA Approaches Using the Last 5 ns of a 50 ns Molecular Dynamic (ΔG) or the Mean of the Total Length of Five 10 ns Molecular Dynamics (ΔG_{mean}) for the Different X/Bim(BH3) Complexes, with X being the Pro-Survival Proteins Bcl-x_L, Bcl-2, Bcl-w, Mcl-1, and Bfl-1[a]

	X				
	Bcl-x_L	Bcl-2	Bcl-w	Mcl-1	Bfl-1
ΔG_{PB}	−63.67	−56.58	−43.40	−44.32	−24.20
$\Delta G_{PB,mean}$	−53.78	−52.83	−16.74	−53.06	−33.03
ΔG_{GB}	−52.10	−50.13	−39.07	−38.35	−17.31
$\Delta G_{GB,mean}$	−48.29	−50.90	−13.74	−47.83	−28.14
K_i (nM)	1.3 ± 0.4	1.4 ± 0.6	2.1 ± 0.3	1.9 ± 0.3	2 ± 0.1

[a]Experimental K_i values were obtained from Dutta et al.[18]

Bim(BH3) and Mcl-1/Bim(BH3) complexes, both coming from X-ray structures, exhibit a very fast convergence. However, 20 ns is needed to achieve the convergence in the Bfl-1/Bim(BH3) complex, also coming from a X-ray structure. The Bcl-2/Bim(BH3) and Bcl-w/Bim(BH3) complexes, obtained by homology modeling, also have different behavior. The first one presents a fast convergence of the binding energy values, although with some fluctuations, whereas the second needs 25 ns to become stable. It is probable that the high sequence homology existing between Bcl-x_L and Bcl-2 proteins leads to an appropriate protein model, whereas when starting from different peptides, even having a good positioning, optimal binding interactions and binding energy convergence are harder to achieve.

Table 1 lists the binding free energy terms corresponding to molecular mechanics and solvation energies (see the Methods) calculated using the MM-PBSA and MM-GBSA approaches for the different X/Bim(BH3) complexes. As can be seen in this table, regardless of the approach used, the total electrostatic contribution (ΔH_{ee} + ΔG_{polar}) to the binding free energy is unfavorable for all of the X/Bim(BH3) complexes studied. In contrast, the van der Waals contribution (ΔH_{vW}) and the nonpolar part of the solvation free energy ($\Delta G_{nonpolar}$) contribute favorably to the binding. Therefore, it is possible to conclude that the favorable binding energy for the formation of the X/Bim(BH3) complexes comes mainly from the nonpolar contributions, as has been previously reported.

The binding free energies calculated for the different X/Bim(BH3) complexes using any of these approaches are situated on a wide energy range of more than 20 kcal/mol, without considering the entropic contribution. The inclusion of this term seems to narrow the energy range, grouping together the binding energies of Bcl-x_L with Bcl-2 and Bcl-w with Mcl-1, isolating the Bfl-1 protein. This trend is more pronounced when using the MMGBSA methodology.

On the other hand, it has recently been suggested that a single long simulation may produce incorrect quantitative results due to inadequate sampling of conformational space, and thus multiple short simulations could better explore the conformational space than a single long simulation.[38] Trying to improve our quantitative results, five 10 ns molecular dynamics was carried out for each system. Within this approach, proteins Bcl-x_L, Bcl-2, and Mcl-1 show a very similar value of their binding free energies, in good agreement with their experimental dissociation constant (Table 2). However, this approach predicts different values for Bcl-w and Bfl-1, with the first being worse and the last being better than the corresponding values for that obtained with single long molecular dynamics. In Figure S1 (Supporting Information), it can be noticed that these two complexes exhibit a different binding free energy profile. The binding energy of the Bcl-w complex decreases along the molecular dynamics trajectory, reaching the highest values in the beginning of the simulation, and, contrarily, the Bfl-1 complex begins with a lowest binding free energy and is increased during the trajectory, leading to a more unfavorable binding free energy value in the long molecular dynamics sampling. Values of ΔG for all of the 10 ns molecular dynamics and for all of the studied systems are included in Tables S8 and S9 of the Supporting Information.

This different behavior of ΔG_{mean} can be expected considering the original structural data of the different Bim complexes. As discussed above, binding energy values obtained for X-ray structures rapidly converge, as well as the Bcl-2 model due to its similarity with the model template used. Thus, values predicted from multiple short molecular dynamics are very close to the ones obtained from single long trajectories. Contrarily, modeled complexes need long simulation times to achieve structural rearrangements and then binding energy convergence. Concretely, these two complexes needed 25 and 20 ns of molecular dynamics, respectively, to achieve ΔG convergence, and thus if we stop the molecular dynamics at 10 ns, structural convergence has not been achieved, and predictions of the binding energy obtained under different approaches may differ. In the case of the Bcl-w complex, the Bim peptide has been modeled, and then it can be expected that binding energy improves as structural rearrangements take place, allowing that the peptide establishes the optimal interactions. On this basis, the descendent trend observed in the binding energy profile can be easily explained. On the other hand, in the Bfl-1 complex, only a protein loop has been modeled, and it is not involved in the peptide binding. For this reason, ΔG differences in this complex are not as remarkable as in the Bcl-w case, and a clear trend cannot be observed in the binding free energy profile.

In conclusion, it can be said that multiple short molecular dynamics lead to better quantitative results, but some considerations must be taken into account before performing binding energy predictions. A better molecular sampling is obtained from multiple dynamics, and so average values obtained from this approach should be better than the ones obtained from a single trajectory. However, for not converged structures, short dynamics will lead to an improper molecular sampling as complex structure cannot converge in short simulation times. In these cases, the single long molecular dynamics simulation is advised.

Residues of Bim(BH3) Critical for Complex Formation. Like in other reported 3D structures of complexes formed between anti- and proapoptotic proteins, in the X/Bim(BH3)

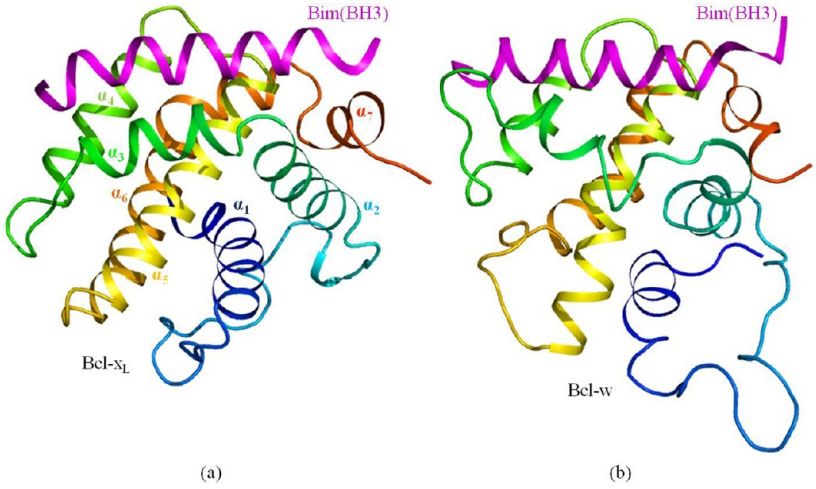

Figure 1. Helical structures of the (a) Bcl-x_L/Bim(BH3) and (b) Bcl-w/Bim(BH3) complexes extracted from the last nanoseconds of the molecular dynamics trajectories.

							P1				P2			P3			P4				P5		
Bim/Bod	53	**R**	**P**	**E**	**I**	**W**	**I**	**A**	**Q**	**E**	**L**	**R**	**R**	**I**	**G**	**D**	**E**	**F**	**N**	**A**	**Y**	**Y**	**A**	74
Bad	105	W	A	A	Q	R	Y	G	R	E	L	R	R	M	S	D	E	F	V	D	S	F	K	126
Bak	69	S	T	M	G	Q	V	G	R	Q	L	A	I	I	G	D	D	I	N	R	R	Y	D	90
Bax	54	A	S	T	K	K	I	S	E	D	L	K	R	I	G	D	E	L	D	S	N	M	E	75
Beclin-1	107	G	T	M	E	N	L	S	R	R	L	K	V	T	G	D	L	F	D	I	M	S	G	128
Bid	81	D	I	I	R	N	I	A	R	H	L	A	Q	V	G	D	S	M	D	R	S	I	P	102
Bik/Nbk	52	E	G	S	D	A	L	A	L	R	L	A	C	I	G	D	E	M	D	V	S	L	R	73
Bmf	63	Q	A	E	V	Q	I	A	R	K	L	Q	C	I	A	D	Q	F	H	R	L	H	R	84
Bok/Mtd	63	G	R	L	A	E	V	C	T	V	L	L	R	L	G	D	E	L	E	Q	I	R	P	84
Hrk/DP5	28	S	A	A	Q	L	T	A	A	R	L	K	A	I	G	D	E	L	H	R	Q	T	M	49
Noxa	20	E	L	E	V	E	C	A	T	Q	L	R	R	F	G	D	K	L	N	F	R	Q	K	41
Puma	122	Q	W	A	R	E	I	G	A	Q	L	R	R	M	A	D	D	L	N	A	Q	Y	E	153

Figure 2. Alignment of the BH3 domain of Bim and other BH3-containing Bcl-2 family members. P1, P2, P3, P4, and P5, depicted in yellow, indicate the relative position of the five conserved hydrophobic residues of the BH3 domains. The aspartic residue of the conserved GD doublet of the BH3 domains is shown in gray.

complexes, the peptide containing the BH3 domain of Bim forms an α-amphipathic helix that binds into the groove that the antiapoptotic protein exposes on its surface. This groove, flanked by the helixes α2, α3, α4, α5, and α8 of the loops connecting these helixes (Figure 1), is predominantly hydrophobic. It is characterized by the presence of four or five small hydrophobic pockets on its surface, in which the side chains of the hydrophobic residues positioned at P1−P4/P5 of the Bim(BH3) peptide sequence are buried (Figures 2 and 3). However, although all of the X/Bim(BH3) complexes studied in the present work share the same binding pattern, differences in the nature of the residues of the antiapoptotic proteins lining the binding site may affect the electrostatic and topological properties of their surfaces and, consequently, the binding properties of Bim(BH3). So, we expect a redistribution of the specific interactions between this peptide and the different antiapoptotic partners.

Bcl-x_L/Bim(BH3) Complex. Residues of Bim(BH3) that contribute to the binding free energy of the Bcl-x_L/Bim(BH3) complex are shown in Figure 4. Of them, residues located at P2, P2+1, and P4 positions of the peptide sequence make the largest contribution to the stability of the complex. The results obtained for the P2 residue are in good agreement with those obtained by Boersma et al.,[39] showing that the mutation [Ala^{P2}]-Bim(BH3) causes a large drop in the affinity for Bcl-x_L. Similarly, Fesik's group demonstrated that the substitution [Ala^{P2}]-Bak(BH3) impairs the binding of this peptide to Bcl-x_L.[8]

In the Bcl-x_L/Bim(BH3) complex, the peptide residue P2+1 is hydrogen bonded to the carbonyl oxygen of Glu^{129} from the protein (Figure 5a; see Supporting Information Table S7). This interaction has been also reported for other Bcl-x_L/BH3-peptide complexes, such those formed by the protein and Beclin-1(BH3)[40,41] or Bad(BH3).[7] However, the large contribution of this residue to the complex stability not only arises from electrostatic interactions, but also from van der Waals contacts (see Supporting Information Table S1). In fact, the side chain of this peptide residue interacts with the side chain of Leu^{130} from Bcl-x_L. This result is in agreement with experimental data showing that the presence of a positively charged residue at P2+1 position does not seem to be critical for Bcl-x_L binding, although it may contribute to increase the binding affinity for this protein (Figure 5b) . Accordingly, it has been demonstrated that the substitutions [Ala^{P2+1}]-Bim(BH3),[39] [Ala^{P2+1}]-Bad(BH3),[7] or [Gln^{P2+1}]-Beclin-1(BH3)[40] decrease the ability of these peptides to bind Bcl-x_L, whereas the mutation [Arg^{P2+1}]-Bak(BH3) enhances its binding affinity for the protein[42,43] (Figure 2).

The large contribution of the P4 residue of Bim(BH3) to the stability of the complex may be attributed to the perpendicular

dx.doi.org/10.1021/ci3001666 | J. Chem. Inf. Model. 2012, 52, 2107−2118

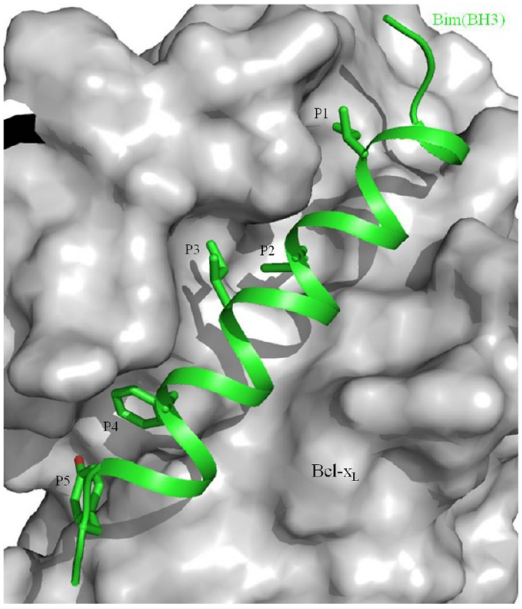

Figure 3. van der Waals surface of Bcl-x_L in its complex with Bim(BH3). In this complex, the side chains of the hydrophobic residues located at P1−P5 of the peptide sequence are projected into the five small hydrophobic pockets spanned over the binding groove surface of the protein.

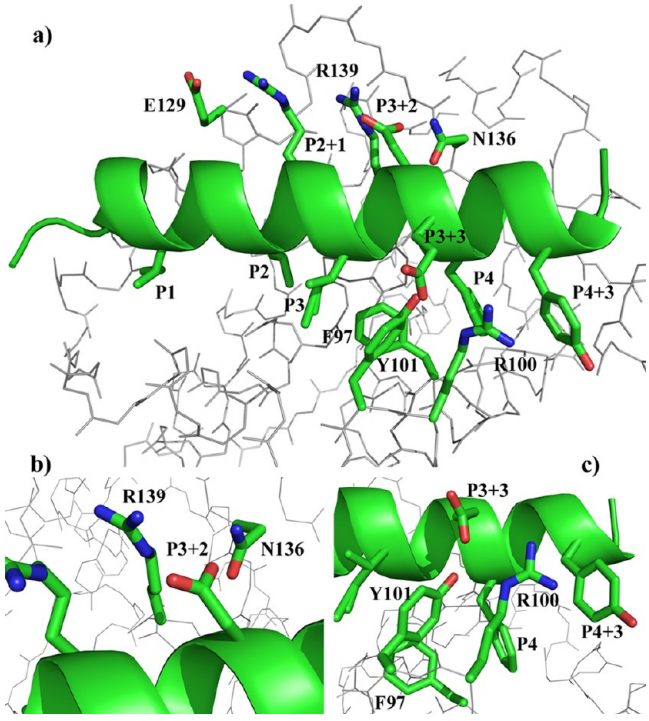

Figure 5. Bcl-x_L-Bim(BH3) interaction pattern. (a) Specific interactions between Bim(BH3) and Bcl-x_L. (b) Close view of the hydrogen bond formed between the residues Arg^{139} and Asn^{136} of Bcl-x_L and the P3+2 residue of Bim(BH3). (c) The aromatic ring of the P4 peptide residue stacks perpendicular against the aromatic moiety of Phe^{97} from Bcl-x_L. Similarly, the P4+3 tyrosine residue forms a parallel staking with the Arg^{100} of Bcl-x_L, which is in turn hydrogen bonded to the P3+3 residue of Bim(BH3).

$\pi-\pi$ stacking interaction between its aromatic moiety and that from Phe^{97} of the protein (Figure 5). The presence of an aromatic or a large hydrophobic residue at the P4 position of the peptide seems to be critical for Bcl-x_L binding, because the substitutions [Ala^{P4}]-Beclin-1^{40} or [Ala^{P4}]-Bim(BH3)[18,19,39] disrupt their binding to the protein. Conversely, the mutation of the threonine at P4 of Beclin-1(BH3) to phenylalanine[40] or the enhancement of the hydrophobicity of the P4 residue in Bak(BH3)[43] increase their affinity for Bcl-x_L. Thus, Bid(BH3) and Bik(BH3) peptides, both characterized by the presence of a methionine residue at the P4 position, bind weakly Bcl-x_L, although in the case of Bid(BH3), it still displays a IC_{50} of 82 nM.[44]

A similar interaction pattern has been found for the Bim(BH3) peptide residue P4+3. In the Bcl-x_L/Bim(BH3) complex, the peptide residue located at P3+3 interacts with the

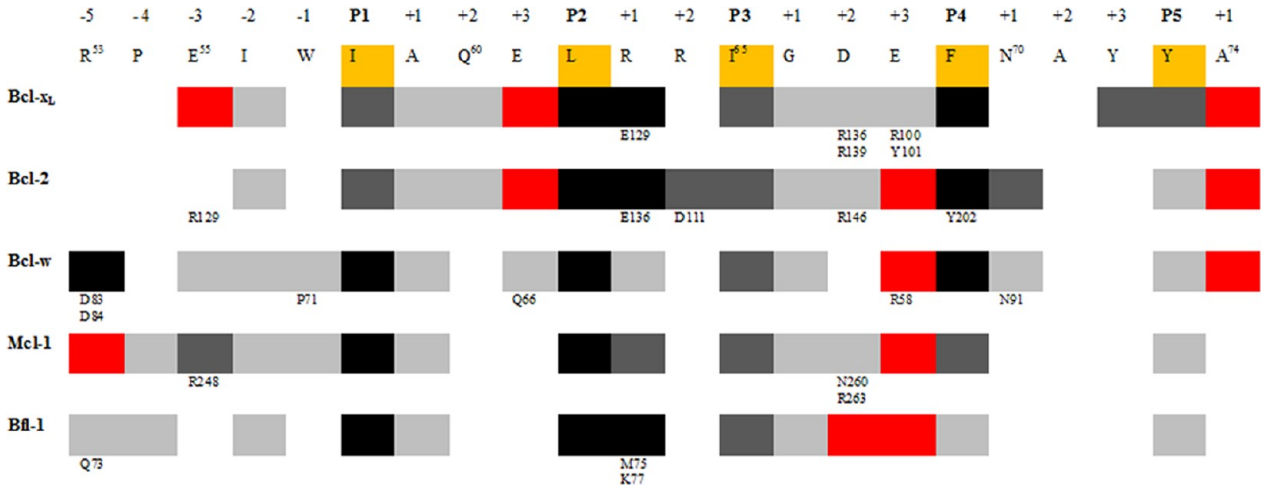

Figure 4. Contribution to the binding free energy of the Bim(BH3) residues in the complexes X/Bim(BH3), where X represents the antiapoptotic proteins Bcl-x_L, Bcl-2, Bcl-w, Mcl-1, and Bfl-1. Residues that contribute unfavorably to the complex formation by more than 0.5 kcal/mol are shown in red, whereas those that favor binding are depicted in gray scale. In this scale, residues that have a contribution larger than 5 kcal/mol to the complex formation are represented in black. Dark gray color has been used for residues having a contribution that ranges from 3 to 5 kcal/mol. Residues whose contribution is equal to or larger than 1.20 kcal/mol and lower than 3 kcal/mol are depicted in light gray. Numbers preceded by a letter indicate residues of X that interact by hydrogen bonding with Bim(BH3).

dx.doi.org/10.1021/ci3001666 | J. Chem. Inf. Model. 2012, 52, 2107−2118

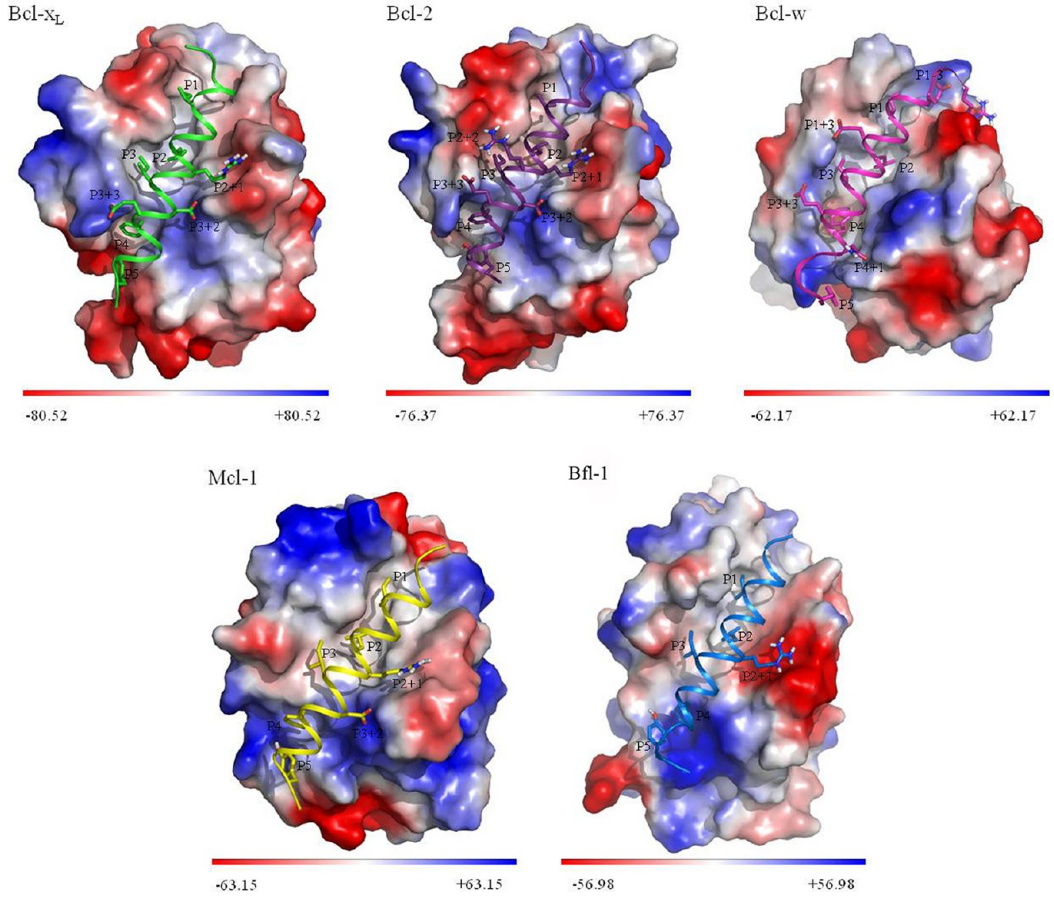

Figure 6. Electrostatic surfaces of the pro-survival proteins Bcl-x$_L$, Bcl-2, Bcl-w, Mcl-1, and Bfl-1 are shown together with a ribbon representation of the Bim(BH3) peptide bound to each one of these proteins. Residues of Bim(BH3) that have the largest electrostatic and van der Waals contributions to the formation of these complexes are labeled. Electrostatic surfaces were calculated using the PyMOL's[49] vacuum electrostatics module.

side chain of the protein residues Arg^{100} and Tyr^{101}. The orientation that adopts the side chain of Arg^{100} in this hydrogen-bond network favors a parallel cation−π stacking interaction with the aromatic moiety of P4+3 (Figure 5). Additional van der Waals interactions provided by the peptide residues P1, P3, and P5 also contribute to stabilize the complex (Figure 5).

The peptide residue P3+2 has been also found important for complex stability. This residue, belonging to the conserved GD doublet of the BH3 domains, is hydrogen bonded to Asn^{136} and Arg^{139} from Bcl-x$_L$ (Figure 5). The stabilizing role of this residue has been pointed out by Sattler and co-workers,[8] who demonstrated that the mutation [Ala^{P3+2}]-Bak(BH3) abrogates its binding to Bcl-x$_L$. Similarly, it has been reported that the substitution [Ala^{P3+2}]-Beclin-1(BH3) disrupts complex formation.[40]

The residues of Bim(BH3) located at P1−3, P1+3, and P5+1 positions of the peptide sequence do not seem to contribute favorably to the binding free energy of the complex (Figure 4).

Bcl-2/Bim(BH3) Complex. Residues of Bim(BH3) that contribute to the binding free energy associated with the formation of its complex with Bcl-2 are essentially the same as those found for the Bcl-x$_L$/Bim(BH3) complex. The exceptions are the peptide residues P2+2, P3+3, P4+3, and P5 (Figure 4).

In the Bcl-2/Bim(BH3) complex, the arginine located at the P2+2 position of the peptide sequence is stabilized by the formation of a hydrogen bond with the protein residue Asp^{111}. This stabilizing interaction has not been observed in the Bcl-x$_L$/Bim(BH3) due to the hydrophobic nature of the residue corresponding to the Asp^{111} of Bcl-2 (Ala^{104} for Bcl-x$_L$) (see Supporting Information Figure S2). However, the presence of a positively charged residue at the P2+2 position seems to be not critical for Bcl-2 binding, because Bak(BH3) or Hrk(BH3) has an hydrophobic residue at this position, and both bind to this protein with high affinity (Figure 4). These observations suggest that the presence of a positively charged residue at the P2+2 position of the peptide sequence may contribute to increase the affinity of the peptides for Bcl-2 over Bcl-x$_L$.

The drop in contribution of the residue located at P4+3 may be attributed to a restructuration of the C-terminal end of the peptide. In the Bcl-2/Bim(BH3) complex, the side chain of this residue is more solvent exposed, thereby reducing its intermolecular contacts. Conversely, the orientation that adopts the side chain of the Bim(BH3) residue P5 favors a parallel $\pi-\pi$ stacking between its aromatic ring and that of the residue Tyr^{202} from Bcl-2, increasing the contribution of this peptide residue to the free energy of the complex.

Finally, residues of Bim(BH3) that contribute unfavorably to the binding free energy of the complex are P1−5, P1−3, P1+3, P3+3, and P5+1, most of them also observed to contribute negatively to the Bcl-x$_L$/Bim(BH3) complex formation (Figure 4; see Supporting Information Table S2).

Bcl-w/Bim(BH3) Complex. The structural rearrangements observed in the Bcl-w protein upon Bim(BH3) binding differ

dx.doi.org/10.1021/ci3001666 | J. Chem. Inf. Model. 2012, 52, 2107−2118

from those observed for the Bcl-x_L or Bcl-2 proteins. Binding of this peptide to Bcl-w unfolds partially the α-helixes α1, α2, α3, α4, and α6 of the protein, although it does not modify the folding of the central hydrophobic helix α5 (Figure 1). As a consequence of these structural rearrangements and the amino acid sequence of Bcl-w, the topology and electrostatic properties of the binding groove of Bcl-w differs from those observed for the Bcl-x_L or Bcl-2 proteins. As can be seen in Figure 6, it is wider and more electropositive, especially at the N- and C-terminus regions of Bim(BH3). As a consequence of this, the orientation that adopts the Bim(BH3) peptide into the Bcl-w binding groove differs significantly from that observed for the Bcl-x_L or Bcl-2 complexes (Figure 7).

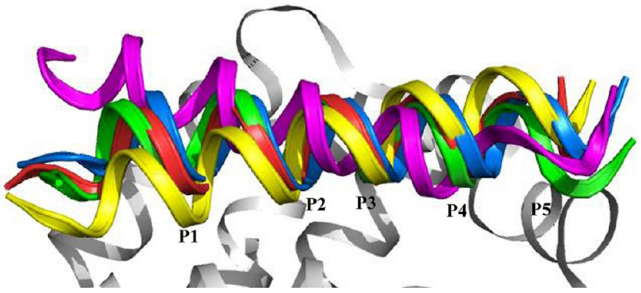

Figure 7. Comparison of the orientation that adopts Bim(BH3) into the binding site of the antiapoptotic proteins Bcl-x_L (green), Bcl-2 (red), Bcl-w (fuchsia), Mcl-1 (blue), and Bfl-1 (yellow).

However, despite these differences, the residues of Bim(BH3) that make the largest contribution to its binding with Bcl-w are essentially the same as those found for the Bcl-x_L or Bcl-2 complexes, although there are some important differences (Figure 4). These differences can be summarized as follows: (1) the residues P1−5, P1−3, and P1+3 of Bim(BH3) contribute favorably to the binding; (2) the Bim(BH3) residues P2+1, P2+2, and P3+2 do not participate in hydrogen bonding with the protein, decreasing their binding contribution to Bcl-w binding; (3) the contribution of the peptide residues P1 to the binding free energy of the complex is enhanced; and (4) the energetic contribution of the peptide residues P1+2 and P4+3 is negligible.

The structural arrangements induced in the α3 helix and the loop connecting α3 and α4 upon Bim(BH3) binding modify the distribution of specific interactions at the N-terminus of the peptide (Figure 1). So, unlike Bcl-x_L and Bcl-2 complexes, the peptide residues P1−5, P1−3, and P1+3 favor the complex formation. Their contribution arises from both van der Waals contacts and electrostatic interactions being hydrogen bonded to Asp^{83}, Glu^{84}, Arg^{77}, and Pro^{71} of Bcl-w, respectively.

In the Bcl-w/Bim(BH3) complex, there is also a loss of the hydrogen bond formed between the P2+1 residue of Bim(BH3) and the Bcl-w residue corresponding to Glu^{129} of Bcl-x_L or Glu^{136} of Bcl-2. Although this residue is also a glutamic in the Bcl-w sequence (Glu^{84}) (see Supporting Information Figure S2), the different orientation of the Bim(BH3) peptide into the binding groove of the protein impairs the formation of this hydrogen bond. As a consequence, there is a drop of the energetic contribution of the Bim(BH3) residue P2+1 to the Bcl-w binding.

One of the most relevant features found in this study is the absence of interaction between the P3+2 aspartic residue from the conserved GD doublet of Bim(BH3) and Bcl-w. In this complex, the side chain of this residue is oriented away from the binding site of the protein, making negligible its contribution to Bcl-w binding. This result differs from those obtained by Denisov et al. for the Bcl-w/Bid(BH3) complex,[25] which found the P3+2 residue of the peptide bound to the Bcl-w residue Arg^{94}. Differences in the results presented in this work can be attributed to the use of different methodologies to characterize these complexes. Whereas the 3D structure of Bcl-w with a bound Bid(BH3) peptide was determined using NMR spectroscopy and molecular docking,[25] we used this complex as a template to build by homology the Bcl-w/Bim(BH3) complex.

The Bim(BH3) residue P3+3 contributes unfavorably to Bcl-w binding due to desolvation effects (see Supporting Information Table S3). Although it is hydrogen bonded to Arg^{58} from Bcl-w, this interaction is not sufficient to compensate the unfavorable effects of desolvation. It is important to note that this residue lacks the hydrogen-bond interaction observed in the Bcl-x_L- and Bcl-2/Bim(BH3) complexes with the Tyr^{101} and Tyr^{108}, respectively. It is because the position of the Bcl-w sequence corresponding to these tyrosine residues is occupied by a phenylalanine (Phe^{56}) (see Supporting Information Figure S2), which stacks perpendicularly against the aromatic moiety of the Bim(BH3) residue located at P4.

Last, the negligible contribution of the Bim(BH3) residue P4+3 to the binding free energy is caused by the lack of helical structure at the C-terminal end of the peptide that orients this residue into the solvent (Figure 1). However, this point should be taken with caution due to the reduced length of the Bim(BH3) peptide. A larger peptide should be studied to better understand the contribution of the terminal residues to the free binding energy of the complex.

If we look carefully at the binding free energy profile for the simulation of this system (see Supporting Information Figure S1), three differentiated intervals can be observed: from 5 to 12 ns, from 12 to 25 ns, and from 25 to 50 ns. To gain insight into the structural changes produced during molecular dynamics, these three intervals were analyzed using the energy decomposition methodology. In Table S10 (Supporting Information), it can be seen that, when going from the first interval to the second one, the most important changes come from the rearrangement of hydrophobic residues. Despite being well positioned from the beginning of the molecular dynamics simulation, some structural changes are necessary to optimize their interactions. This change in the contribution of the hydrophobic residues to the binding free energy also appears when going from the second to the third interval, but with a smaller range. The hydrogen-bond network in the first time period analyzed is constituted only by Arg^{53} and Asn^{70} residues. However, hydrogen bonds for both residues disappear in the second interval, being recovered again in the last interval (see Supporting Information Tables S7 and S11). The optimal hydrogen-bond network, including the contribution of the above-mentioned Glu aminoacids, is achieved in the third interval. Thus, the increase of the hydrophobic contributions together with the changes is hydrogen bonds network are in good agreement with the free energy convergence behavior observed for the Bcl-w/Bim(BH3) complex.

Mcl-1/Bim(BH3) Complex. The orientation that Bim(BH3) adopts bound into the binding groove of Mcl-1 is very similar to that observed in the Bcl-x_L- and Bcl-2/Bim(BH3) complexes (Figure 7). This result was unexpected in view of the

electrostatic and topological properties of the Mcl-1 binding groove. In contrast to Bcl-x_L, Bcl-2, or Bcl-w, the binding groove of Mcl-1 is more open and more positively charged, especially in the region located at the C-terminus of the peptide (Figure 6). These properties confer to Mcl-1 some features that are different among these antiapoptotic proteins. These features are (Figure 4): (1) there is a reinforcement of the contribution of the Bim(BH3) residues P1−1, P1−3, and P1−4 to the binding free energy; (2) the energetic contribution of the Bim(BH3) residue P3+3 to the complex formation is negligible; and (3) there is a drop in contribution of the peptide residue P4 to Mcl-1 binding.

Unlike the Bcl-x_L-, Bcl-2-, and Bcl-w/Bim(BH3) complexes, in the Mcl-1/Bim(BH3) complex the side chains of the peptide residues P1−1 and P1−4 are oriented toward the binding site, showing significant interactions with the side chains of nearby Mcl-1 residues.

One of the most relevant features found for the Mcl-1/Bim(BH3) is the drop in contribution of the peptide residue P4 to Mcl-1 binding. In the Bcl-x_L- and Bcl-2/Bim(BH3) complexes, the aromatic moiety of this residue packs against Phe^{97} and Phe^{101} from Bcl-x_L and Bcl-2, respectively, which are replaced by a valine in Mcl-1 (Val^{220}) (see Supporting Information Figure S2). Consequently, the $\pi-\pi$ stacking is lost, and the energetic contribution of the Bim(BH3) residue P4 to the Mcl-1 binding is decreased (see Supporting Information Table S4). This finding suggests that the presence of a large hydrophobic or aromatic residue at the P4 position may not increase significantly the affinity of the BH3 peptide for Mcl-1. It is in agreement with previous experimental studies showing that the mutation [Ala^{P4}]-Bim(BH3) has only a minimal impact on Mcl-1 binding.[18,39]

In the Mcl-1/Bim(BH3) complex, the P2+1 residue is hydrogen bonded to the oxygen carbonyl of the Mcl-1 residue corresponding to Glu^{129}/Glu^{136} from Bcl-x_L/Bcl-2 (His^{252}) (see Supporting Information Figure S2), although its energetic contribution comes also from the van der Waals contacts with the neighboring residues. Moreover, like the Bcl-x_L- and Bcl-2/Bim(BH3) complexes, the P3+2 residue from the conserved GD doublet forms a hydrogen bond with the protein residues corresponding to Asn^{136} and Arg^{139} from Bcl-x_L (residues Asn^{260} and Arg^{263} from Mcl-1, respectively). The formation of a hydrogen bond between the Bim(BH3) residue P3+2 and Arg^{263} of Mcl-1 has been also reported by Czabotar et al.[22] and found in the complex Mcl-1/Bax.[45]

For all of the studied systems, an open question arises about the possibility that, even being in the zone of the molecular dynamics interval with converged binding free energy, the quantitative description introduced by the energy decomposition methodology could be biased by simulation period considered for the sampling. To assess this question, we selected the Mcl-1/Bim(BH3) system. Our selection was based on the fact that the binding free energy of this system (see Supporting Information Figure S1) present some fluctuations in the last two 5 ns intervals (from 40 to 45 ns and from 45 to 50 ns), suggesting some differences in the peptide−protein interaction. To analyze the binding pattern differences in these two intervals, binding free energy decomposition was calculated, and, as can be observed when comparing Supporting Information Tables S4 and S5, both results are almost identical.

Bfl-1/Bim(BH3) Complex. The orientation that adopts Bim(BH3) into the binding site of Bfl-1 slightly differs from that observed in the Bcl-x_L-, Bcl-2-, and Mcl-1/Bim(BH3) complexes (Figure 7). One of the most direct consequences is that the conserved aspartic residue located at P3+2 of the peptide sequence is not involved in any intermolecular hydrogen bond. On the other hand, residues of Bim(BH3) located at P1, P2, and P2+1 positions have the largest contribution to the complex formation (Figure 4).

The lack of hydrogen bond between the P3+2 residue of Bim(BH3) and Bcl-w is not in agreement with the results obtained by the Nordlund's group,[21] who reported the formation of a hydrogen bond between this peptide residue and the Arg^{88} of Bfl-1 in the crystal structure of this complex. In contrast, we observed the loss of this interaction during the molecular dynamics simulation. It can be attributed to the use of higher temperatures during the MD trajectories in comparison with that used in X-ray crystallography.

In this complex, the P2+1 residue is hydrogen bonded to the oxygen carbonyl of the Bfl-1 residues Met^{75} and Lys^{77}, respectively. These interactions show correspondence with those observed in the Bcl-x_L, Bcl-2, and Mcl-1/Bim(BH3) complexes between the peptide residue P2+1 and the protein residues Glu^{129}, Glu^{136}, and His^{252}, respectively. Although this interaction has not been found in the complex Bcl-w/Bim(BH3), it is interesting to note that the Bcl-w residue corresponding to those of Bcl-x_L, Bcl-2, or Mcl-1 forms a hydrogen bond with the Bim(BH3) peptide residue P1−5. Taken together, these results suggest that the position that is occupied by the residue Glu^{129} in the Bcl-x_L protein plays a critical role in the binding of BH3 peptide domains to the antiapoptotic Bcl-2 family members.

Bcl-w also presents a phenylalanine residue (Phe^{42}) at the position of the sequence corresponding to Phe^{97}/Phe^{104} of Bcl-x_L/Bcl-2 (see Supporting Information Figure S2), where these residues stack perpendicular against the aromatic moiety of the P4 peptide residue. In the Bfl-1/Bim(BH3) complex, as in the case of the Mcl-1 complex, this stabilizing interaction does not exist, decreasing the contribution of the P4 residue of Bim(BH3) to the binding free energy of the complex. However, in contrast to Mcl-1, the absence of this interaction in the Bfl-1/Bim(BH3) is due to the restructuration of the Bfl-1 α2 helix upon Bim(BH3) binding, which orients this Phe^{42} away from the binding site.

For this system, the binding free energy profile (see Supporting Information Figure S1) shows two differentiated intervals, one ranging from 5 to 20 ns and other from 20 to 50 ns. To confirm the obtained binding pattern, the contribution of peptide residues was analyzed for the two simulation periods as done for the previous complexes. A different behavior is observed with respect to the Bcl-w complex (see Supporting Information Table S10). In this case, hydrophobic interactions are present from the beginning of the simulation, but there is a decrease in its contribution along the dynamics. On the other hand, the hydrogen-bond network is limited to Arg^{53} and Arg^{63} in the last 5 ns due to the disappearance of the Asp^{67} hydrogen bond (see Supporting Information Tables S7 and S11). As the structure of the binding site was directly obtained from the X-ray data, binding energy values predicted from the beginning of molecular dynamics simulation correspond to the experimental and optimal structure. However, the loop modeling may interfere in the protein structure, deviating it from the optimal structure after simulation. This can be the reason for the significant worsening of the P5 contribution observed in the final interval of the molecular dynamics simulation. However, it is noticeable that, even considering this drop in the P5

contribution, this residue must also be considered as significant for the peptide binding.

CONCLUSIONS

Targeting the whole family of pro-survival Bcl-2 proteins is a promising strategy for designing an effective cancer therapy. Hence, the study of interactions present in the Bim(BH3) peptide complexes with these proteins should give some perspective for designing small molecules that, as Bim(BH3) does, bind the whole set of proteins.

Predictions of binding free energy values have always been a complex issue, especially when structural data of the object systems are not directly obtained from experiment. However, they are a key issue for determining the binding pattern of a given molecule.

In the present work, MM-GB/PBSA methodology was used for this purpose, using different protocols for molecular sampling, which have proven a proper performance. Despite the fluctuations observed in the predictions of these methods, all of the approaches and time intervals analyzed in these work lead to equivalent results.

The binding of Bim(BH3) to the antiapoptotic proteins Bcl-x_L, Bcl-2, Bcl-w, Mcl-1, and Bfl-1 is mainly governed by hydrophobic interactions that arise from the four conserved hydrophobic residues located at the P1−P4 positions of the peptide sequence. The individual contribution of P1 and P4 residues to the total binding energy varies across the series of studied complexes, whereas that of P2 and P3 remains stable throughout it (Figure 4).

The P2 residue is one of the most contributing residues to the formation of the X/Bim(BH3) complexes (>5 kcal/mol). The P2 position is occupied by a leucine that is conserved in all BH3-containing proteins identified to date. The critical role of this residue in protein binding has been demonstrated by previous experimental studies showing that mutations of this conserved residue disrupt the binding of BH3 peptides to antiapoptotic Bcl-2 family members.[8,15,39,40,46,47] In contrast, the contribution of the P4 residue to Bcl-x_L, Bcl-2, and Bcl-w binding is 2 kcal/mol greater than that obtained for Mcl-1 or Bfl-1, whereas the contribution of the P1 residue to Bcl-w, Mcl-1, or Bfl-1 complex formation exceeds in ∼1 kcal/mol that obtained for Bcl-x_L or Bcl-2. Taken together, these findings suggest that the P1 and P4 peptide residues do not only contribute to the stability of the X/Bim(BH3) complexes, but may also play some role in determining the binding selectivity of Bim(BH3) and other BH3 peptides for antiapoptotic proteins. A proof of this concept is that Bad(BH3) has not measurable binding to Mcl-1 and Bfl-1, whereas the substitution [Ile^{P1}]-Bad(BH3) yields a peptide able to bound all five antiapoptotic Bcl-2 family members.[48] However, the amino acid composition at the P1 and P4 positions of the peptide sequence may not be the only factor involved in binding selectivity, because Bmf(BH3) shares the same amino acid residues as Bim(BH3) at these positions, but it binds weakly Mcl-1 and Bfl-1.[14]

Although the binding of Bim(BH3) to antiapoptotic proteins is mainly hydrophobic, electrostatic interactions may also contribute to complex formation in different ways. At long distances, they may be involved in the recognition of the Bim(BH3) peptide by antiapoptotic proteins (selectivity) and in the attainment of the correct orientation to form the complexes. At short distances, the electrostatic interactions between X and Bim(BH3) may contribute to increase the binding strength.

In the X/Bim(BH3) complexes, the electrostatic contribution of individual peptide residues seems to depend on the sequence of the interacting partner. Thus, the aspartic residue of the conserved GD doublet of Bim(BH3) has been found critical for Bcl-x_L, Bcl-2, and Mcl-1 binding, but it seems to be not required for Bcl-w or Bfl-1 binding. In these complexes, the side chain of this aspartic residue is oriented toward the solvent, making negligible its contribution to complex formation. This result was unexpected taking into account the complete conservation of this residue among the Bcl-2 family members, but opens the door to a new perspective: at large distances, the sequence containing the conserved GD doublet of BH3 domains acts as an essential and efficient motif for X-Bim(BH3) recognition; at short distances, the formation of a hydrogen bond between the aspartic residue of the GD doublet and X depends on the electrostatic properties of the binding groove.

Another important feature found in the present work is that, although the Bim(BH3) interacting residues are fully distributed along the peptide sequence, the C-terminal interactions seem to be stronger for the Bcl-x_L and Bcl-2 than for the Mcl-1 or Bfl-1 proteins. In contrast, for the last ones, the N-terminal interactions appear to be more important, with Bcl-w being an intermediate case between these two cases.

Taken together, these findings clearly point out the difficulty of designing Bim(BH3) mimetics able to target all antiapoptotic proteins, because the contribution of each peptide residue to the binding free energy of these complexes seems to depend not only on the interacting protein, but also on the neighboring residues of the peptide sequence. Both factors may determine the binding specificity of peptides based on the BH3 domain of proapoptotic members toward pro-survival proteins. However, despite this, results obtained in the present work suggest that two hydrophobic groups mimicking the P2 and P3 residues of Bim(BH3) and a negative charge mimicking the P3+2 residue should be the minimal common requirements for X binding. Incorporation of additional groups to this pharmacophoric model might improve the affinity of these BH3-mimetics by X, although this increment may be dependent on the X type. For example, it is expected that the addition of a positive charge at the P3+3 position might improve the affinity of these compounds for Bcl-x_L and Bcl-2 over the remaining antiapoptotic members.

ASSOCIATED CONTENT

Supporting Information

Total binding free energy of the X/Bim(BH3) complexes, where X represents the antiapoptotic proteins Bcl-xL, Bcl-2, Bcl-w, Mcl-1, and Bfl-1; the contribution of the Bim(BH3) residues to the binding free energy of the Bcl-x_L/Bim(BH3) complexes; MM-GBSA and MM-PBSA total binding free energies for the five 10 ns molecular dynamics of these complexes; the hydrogen bonds formed between Bim(BH3) and X; contribution of the Bim(BH3) residues to the binding free energy of the Bcl-w/Bim(BH3) and Bfl-1/Bim(BH3) complexes averaged over different intervals of the molecular dynamics; hydrogen bonds formed between Bim(BH3) and Bcl-w at different intervals of the molecular dynamics; and sequence alignment of the pro-survival proteins Bcl-x_L, Bcl-2, Bcl-w, Mcl-1, and Bfl-1. This material is available free of charge via the Internet at http://pubs.acs.org.

AUTHOR INFORMATION

Corresponding Author

*Phone: (+34) 93 4039263. Fax: (+34) 93 4021231. E-mail: jaime.rubio@ub.edu.

Notes

The authors declare no competing financial interest.

ACKNOWLEDGMENTS

This work was supported by Ministerio Español de Ciencia y Tecnologia (project CTQ2011-29285-C02-02) and the Generalitat of Catalunya (project 2009SGR1308). We are also grateful to the Departament d'Universitat, Recerca i Societat de la Informacio de la Generalitat de Catalunya i del Fons Social Europeu. We thankfully acknowledge the computer resources, technical expertise, and assistance provided by the Barcelona Supercomputing Center - Centro Nacional de Supercomputación, under the project "Understanding protein−protein interactions: towards the design of inhibitors for the Bcl-2 protein family".

REFERENCES

(1) Youle, R. J.; Strasser, A. The Bcl-2 protein family: opposing activities that mediate cell death. *Nat. Rev. Mol. Cell Biol.* **2008**, *9*, 47−59.

(2) Green, D. R.; Evan, G. I. A matter of life and death. *Cancer Cell* **2002**, *1*, 19−30.

(3) Hanahan, D.; Weinberg, R. A. The hallmarks of cancer. *Cell* **2000**, *100*, 57−70.

(4) Leber, B.; Geng, F.; Kale, J.; Andrews, D. W. Drugs targeting Bcl-2 family members as an emerging strategy in cancer. *Expert Rev. Mol. Med.* **2010**, *12*, e28.

(5) Reed, J. C. Mechanisms of apoptosis. *Am. J. Pathol.* **2000**, *157*, 1415−1430.

(6) Liu, X.; Dai, S.; Zhu, Y.; Marrack, P.; Kappler, J. W. The structure of a Bcl-x_L/Bim fragment complex: implications for Bim function. *Immunity* **2003**, *19*, 341−352.

(7) Petros, A. M.; Nettesheim, D. G.; Wang, Y.; Olejniczak, E. T.; Meadows, R. P.; Mack, J.; Swift, K.; Matayoshi, E. D.; Zhang, H.; Thompson, C. B.; Fesik, S. W. Rationale for Bcl-x_L/Bad peptide complex formation from structure, mutagenesis, and biophysical studies. *Protein Sci.* **2000**, *9*, 2528−2534.

(8) Sattler, M.; Liang, H.; Nettesheim, D.; Meadows, R. P.; Harlan, J. E.; Eberstadt, M.; Yoon, H. S.; Shuker, S. B.; Chang, B. S.; Minn, A. J.; Thompson, C. B.; Fesik, S. W. Structure of Bcl-x_L-Bak peptide complex: recognition between regulators of apoptosis. *Science* **1997**, *275*, 983−986.

(9) Cosulich, S. C.; Worrall, V.; Hedge, P. J.; Green, S.; Clarke, P. R. Regulation of apoptosis by BH3 domains in a cell-free system. *Curr. Biol.* **1997**, *7*, 913−920.

(10) Letai, A.; Bassik, M. C.; Walensky, L. D.; Sorcinelli, M. D.; Weiler, S.; Korsmeyer, S. J. Distinct BH3 domains either sensitize or activate mitochondrial apoptosis, serving as prototype cancer therapeutics. *Cancer Cell* **2002**, *2*, 183−192.

(11) Kuwana, T.; Bouchier-Hayes, L.; Chipuk, J. E.; Bonzon, C.; Sullivan, B. A.; Green, D. R.; Newmeyer, D. D. BH3 domains of BH3-only proteins differentially regulate Bax-mediated mitochondrial membrane permeabilization both directly and indirectly. *Mol. Cell* **2005**, *17*, 525−535.

(12) Holinger, E. P.; Chittenden, T.; Lutz, R. J. Bak BH3 peptides antagonize Bcl-x_L function and induce apoptosis through cytochrome c-independent activation of caspases. *J. Biol. Chem.* **1999**, *274*, 13298−13304.

(13) Bajwa, N.; Liao, C.; Nikolovska-Coleska, Z. Inhibitors the anti.apoptotic Bcl-2 proteins: a patent review. *Expert Opin. Ther. Pat.* **2012**, *22*, 37−55.

(14) Chen, L.; Willis, S. N.; Wei, A.; Smith, B. J.; Fletcher, J. I.; Hinds, M. G.; Colman, P. M.; Day, C. L.; Adams, J. M.; Huang, D. C. Differential targeting of prosurvival Bcl-2 proteins by their BH3-only ligands allows complementary apoptotic function. *Mol. Cell* **2005**, *17*, 393−403.

(15) Oltersdorf, T.; Elmore, S. W.; Shoemaker, A. R.; Armstrong, R. C.; Augeri, D. J.; Belli, B. A.; Bruncko, M.; Deckwerth, T. L.; Dinges, J.; Hajduk, P. J.; Joseph, M. K.; Kitada, S.; Korsmeyer, S. J.; Kunzer, A. R.; Letai, A.; Li, C.; Mitten, M. J.; Nettesheim, D. G.; Ng, S.; Nimmer, P. M.; O'Connor, J. M.; Oleksijew, A.; Petros, A. M.; Reed, J. C.; Shen, W.; Tahir, S. K.; Thompson, C. B.; Tomaselli, K. J.; Wang, B.; Wendt, M. D.; Zhang, H.; Fesik, S. W.; Rosenberg, S. H. An inhibitor of Bcl-2 family proteins induces regression of solid tumours. *Nature* **2005**, *435*, 677−681.

(16) van Delft, M. F.; Wei, A. H.; Mason, K. D.; Vandenberg, C. J.; Chen, L.; Czabotar, P. E.; Willis, S. N.; Scott, C. L.; Day, C. L.; Cory, S.; Adams, J. M.; Roberts, A. W.; Huang, D. C. The BH3 mimetic ABT-737 targets selective Bcl-2 proteins and efficiently induces apoptosis via Bak/Bax if Mcl-1 is neutralized. *Cancer Cell* **2006**, *10*, 389−399.

(17) Chauhan, D.; Velankar, M.; Brahmandam, M.; Hideshima, T.; Podar, K.; Richardson, P.; Schlossman, R.; Ghobrial, I.; Raje, N.; Munshi, N.; Anderson, K. C. A novel Bcl-2/Bcl-x_L/Bcl-w inhibitor ABT-737 as therapy in multiple myeloma. *Oncogene* **2007**, *26*, 2374−2380.

(18) Dutta, S.; Gullá, S.; Chen, T. S.; Fire, E.; Grant, R. A.; Keating, A. E. Determinants of BH3 binding specificity for Mcl-1 versus Bcl-x_L. *J. Mol. Biol.* **2010**, *398*, 747−762.

(19) Lee, E. F.; Sadowsky, J. D.; Smith, B. J.; Czabotar, P. E.; Peterson-Kaufman, K. J.; Colman, P. M.; Gellman, S. H.; Fairlie, W. D. High-resolution structural characterization of a helical alpha/beta-peptide foldamer bound to the anti-apoptotic protein Bcl-x_L. *Angew. Chem., Int. Ed.* **2009**, *48*, 4318−4322.

(20) Fire, E.; Gullá, V. G.; Grant, R. A.; Keating, A. E. Mcl-1−Bim complexes accommodate surprising point mutations via minor structural changes. *Protein Sci.* **2010**, *19*, 507−519.

(21) Herman, M. D.; Nyman, T.; Welin, M.; Lehtiö, L.; Flodin, S.; Trésaugues, L.; Kotenyova, T.; Flores, A.; Nordlund, P. Completing the family portrait of the anti-apoptotic Bcl-2 proteins: crystal structure of human Bfl-1 in complex with Bim. *FEBS Lett.* **2008**, *582*, 3590−3594.

(22) Czabotar, P. E.; Lee, E. F.; van Delft, M. F.; Day, C. L.; Smith, B. J.; Huang, D. C.; Fairlie, W. D.; Hinds, M. G.; Colman, P. M. Structural insights into the degradation of Mcl-1 induced by BH3 domains. *Proc. Natl. Acad. Sci. U.S.A.* **2007**, *104*, 6217−6222.

(23) Sali, A.; Potterton, L.; Yuan, F.; van Vlijmen, H.; Karplus, M. Evaluation of comparative protein modeling by Modeller. *Proteins: Struct., Funct., Genet.* **1995**, *23*, 318−326.

(24) Fiser, A.; Do, R. K.; Sali, A. Modeling of loops in protein structures. *Protein Sci.* **2000**, *9*, 1753−1773.

(25) Denisov, A. Y.; Chen, G.; Sprules, T.; Moldoveanu, T.; Beauparlant, P.; Gehring, K. Structural model of the BCL-w-BID peptide complex and its interactions with phospholipid micelles. *Biochemistry* **2006**, *45*, 2250−2256.

(26) Case, D. A.; Darden, T.; Cheatham, T. E., III; Simmerling, C.; Wang, J.; Duke, R.; Luo, R.; Merz, K.; Pearlman, D.; Crowley, M.; Walker, R.; Zhang, W.; Wang, B.; Hayik, A.; Roiberg, A.; Seabra, G.; Wong, K.; Paesani, F.; Wu, X.; Brozell, S.; Tsui, V.; Gohlke, H.; Yang, L.; Tan, C.; Morgan, J.; Hornak, V.; Cui, G.; Beroza, P.; Matthews, D.; Schfmeister, C.; Ross, W.; Kollman, P. *AMBER 9*; University of California: San Francisco, CA, 2006.

(27) Jorgensen, W. L.; Chandrasekhar, J.; Madura, J. D.; Impey, R. W.; Klein, M. L. Comparison of simple potential functions for modeling water. *J. Chem. Phys.* **1983**, *79*, 926−935.

(28) Hornak, V.; Abel, R.; Okur, A.; Strockbine, B.; Roitberg, A.; Simmerling, C. Comparison of multiple Amber force fields and development of improved protein backbone parameters. *Proteins* **2006**, *65*, 712−725.

(29) Berendsen, H. J. C.; Postma, J. P. M.; van Gunsteren, W. F.; DiNola, A.; Haak, J. R. Molecular-dynamics with coupling to an external bath. *J. Chem. Phys.* **1984**, *81*, 3684−3690.
(30) Ryckaert, J. P.; Ciccotti, G.; Berendsen, H. J. C. Numerical integration of the cartesian equations of motion of a system with constraints: Molecular dynamics of n-alkanes. *J. Comput. Phys.* **1977**, *23*, 327−341.
(31) Darden, T.; York, D.; Pedersen, L. Particle mesh Ewald-an N.Log(N) method for Ewald sums in large systems. *J. Chem. Phys.* **1993**, *98*, 10089−10092.
(32) Kollman, P. A.; Massova, I.; Reyes, C.; Kuhn, B.; Huo, S. H.; Chong, L.; Lee, M.; Lee, T.; Duan, Y.; Wang, W.; Donini, O.; Cieplak, P.; Srinivasan, J.; Case, D. A.; Cheatham, T. E. Calculating structures and free energies of complex molecules: Combining molecular mechanics and continuum models. *Acc. Chem. Res.* **2000**, *33*, 889−897.
(33) Onufriev, A.; Bashford, D.; Case, D. A. A modification of the generalized born model suitable for macromolecules. *J. Phys. Chem. B* **2000**, *104*, 3712−3720.
(34) Luo, R.; David, L.; Gilson, M. K. Accelerated Poisson-Boltzmann calculations for static and dynamic systems. *J. Comput. Chem.* **2002**, *23*, 1244−1253.
(35) Weiser, J.; Shenkin, P. S.; Still, W. C. Approximate solvent-accessible surface areas from tetrahedrally directed neighbor densities. *Biopolymers* **1999**, *50*, 373−380.
(36) Chen, J.; Im, W.; Brooks, C. L., III. Balancing solvation and intramolecular interactions: toward a consistent generalized Born force field. *J. Am. Chem. Soc.* **2006**, *128*, 3728−3736.
(37) Gohlke, H.; Kiel, C.; Case, D. A. Insights into protein-protein binding by binding free energy calculation and free energy decomposition for the Ras-Raf and Ras-RalGDS complexes. *J. Mol. Biol.* **2003**, *330*, 891−913.
(38) Sadiq, S. K.; Wright, D. W.; Kenway, O. A.; Coveney, P. W. Accurate ensemble molecular dynamics binding free energy ranking of multidrug-resistant HIV-1 proteases. *J. Chem. Inf. Model.* **2010**, *50*, 890−905.
(39) Boersma, M. D.; Sadowsky, J. D.; Tomita, Y. A.; Gellman, S. H. Hydrophile scanning as a complement to alanine scanning for exploring and manipulating protein-protein recognition: application to the Bim BH3 domain. *Protein Sci.* **2008**, *17*, 1232−1240.
(40) Feng, W.; Huang, S.; Wu, H.; Zhang, M. Molecular basis of Bcl-x_L's target recognition versatility revealed by the structure of Bcl-x_L in complex with the BH3 domain of Beclin-1. *J. Mol. Biol.* **2007**, *372*, 223−235.
(41) Oberstein, A.; Jeffrey, P. D.; Shi, Y. Crystal structure of the Bcl-x_L-Beclin 1 peptide complex: Beclin 1 is a novel BH3-only protein. *J. Mol. Biol.* **2007**, *282*, 13123−13132.
(42) Lama, D.; Sankararamakrishnan, R. Anti-apoptotic Bcl-x_L protein in complex with BH3 peptides of pro-apoptotic Bak, Bad, and Bim proteins: comparative molecular dynamics simulations. *Proteins* **2008**, *73*, 492−514.
(43) Frey, V.; Viaud, J.; Subra, G.; Cauquil, N.; Guichou, J. F.; Casara, P.; Grassy, G.; Chavanieu, A. Structure-activity relationships of Bak derived peptides: affinity and specificity modulations by amino acid replacement. *Eur. J. Med. Chem.* **2008**, *43*, 966−972.
(44) Chen, L.; Willis, S. N.; Wei, A.; Smith, B. J.; Fletcher, J. I.; Hinds, M. G.; Colman, P. M.; Day, C. L.; Adams, J. M.; Huang, D. C. Differential targeting of prosurvival Bcl-2 proteins by their BH3-only ligands allows complementary apoptotic function. *Mol. Cell* **2005**, *17*, 393−403.
(45) Czabotar, P. E.; Lee, E. F.; Thompson, G. V.; Wardak, A. Z.; Fairlie, W. D.; Colman, P. M. Mutation to Bax beyond the BH3 domain disrupts interactions with pro-survival proteins and promotes apoptosis. *J. Biol. Chem.* **2011**, *286*, 7123−7131.
(46) Shangary, S.; Johnson, D. E. Peptides derived from BH3 domains of Bcl-2 family members: a comparative analysis of inhibition of Bcl-2, Bcl-x_L and Bax oligomerization, induction of cytochrome c release, and activation of cell death. *Biochemistry* **2002**, *41*, 9485−9495.
(47) Willis, S. N.; Chen, L.; Dewson, G.; Wei, A.; Naik, E.; Fletcher, J. I.; Adams, J. M.; Huang, D. C. Proapoptotic Bak is sequestered by Mcl-1 and Bcl-x_L, but not Bcl-2, until displaced by BH3-only proteins. *Genes Dev.* **2005**, *19*, 1294−1305.
(48) Day, C. L.; Chen, L.; Richardson, S. J.; Harrison, P. J.; Huang, D. C.; Hinds, M. G. Solution structure of prosurvival Mcl-1 and characterization of its binding by proapoptotic BH3-only ligands. *J. Biol. Chem.* **2005**, *280*, 4738−4744.
(49) Delano, W. L. *The PyMOL Molecular Graphics System, Version v.099rc6*; Schrödinger, LLC, 2001.